Isolation and Characteristics of Cellulose and Nanocellulose from Lotus Leaf Stalk Agro-wastes

Yandan Chen,[a,*] Qiaomei Wu,[a] Biao Huang,[a] Mingjie Huang,[b] and Xiaolin Ai [a]

Valorization of lotus leaf stalks (LLS) produced as an abundantly available agro-waste was achieved through the extraction of value-added nanocellulose. Nanofibrillated cellulose (NFC) was successfully prepared from LLS by using chemical pretreatment combined with high-intensity ultrasonication. The morphological characteristics of the chemically purified LLS cellulose microfibrils were characterized by optical microscopy and MorFi fiber analysis. Fourier transform infrared (FTIR) spectroscopy indicated the extensive removal of non-cellulosic components after chemical pretreatment. The transmission electron microscopy (TEM) results revealed agglomeration of the developed individual NFC, with a width of 20 ± 5 nm and length on a micron scale, into a network-like feature. X-ray diffraction results showed that the resulting NFC had a cellulose I crystal structure with a high crystallinity (70%). The NFC started to degrade at around 217 °C, and the peak rate of degradation occurred at 344 °C. Nanofibrils obtained from LLS have great potential as reinforcement agents in nanocomposites.

Keywords: Nanocellulose; Lotus leaf stalk; Ultrasonication; Morphological characteristics; Thermal degradation

*Contact information: a: College of Materials Engineering, Fujian Agriculture and Forestry University, Fuzhou 350002, China; b: College of Life Sciences, Fujian Agriculture and Forestry University, Fuzhou 350002, China; *Corresponding author: fjaucyd@163.com*

INTRODUCTION

Cellulose, a product of the photosynthesis process in plants and trees, is considered the most abundant renewable polymer resource on earth, and is a prime candidate for replacing oil-based feedstocks. The concept of breaking down the hierarchical structure of various species of plant-based cellulose to form its elementary "building blocks" variously termed nanocrystals, nanowhiskers, nanofibrils, and nanofibers, has become a hot topic. This is on the basis of the unique features of cellulose "building blocks" including nanometer-scale dimensions combined with important macroscopic cellulose properties (Eichhorn 2011). Thus, these novel nanocelluloses open up a wide range of possible properties and promising applications (Lin and Dufresne 2014). Top-down methods involving enzymatic/chemical/physical methodologies as well as a combination of the aforementioned methods for nanocellulose isolation from wood and agricultural residues have been widely investigated (Klemm *et al*. 2011; Tang *et al*. 2014). These experimental techniques lead to a variety of nanocelluloses, differing in dimensions, morphologies, and degree of crystallinity depending on the initial biological source and the processing conditions (Haafiz *et al*. 2014).

The possible use of various local seasonal forest or agricultural residues as nanocellulose precursors has recently received increased attention worldwide for their abundance at low cost and for the attempts of valorization (Brinchi *et al*. 2013; Neto *et al*.

2013). It would be more worthwhile to generate nanocelluloses from fast-growing renewable plants than from slow-growing plants with respect to the economic and ecological benefits.

Lotus (*Nelumbo nucifera* Gaertn.) is a perennial water plant originating in India and China (Cheng *et al*. 2013). The lotus plant (Fig. 1a) has long leaf stalks, at which the leaves or flowers are attached to the modified stems. It can grow to a height of up to 6 m, depending on the depth of water. It is an important and popular cash crop widely cultivated in many Asian countries, primarily because of its high edible and medicinal values derived from its rhizomes, seeds, and leaves (Man *et al*. 2012; Cheng *et al*. 2013). The total planting area of lotus in China was estimated to be over 330,000 hectares in 2004 (Xu *et al*. 2013), and it keeps increasing, even today. After harvest, a large amount of lotus leaf stalks (LLS) are normally generated as waste and abandoned for natural decay, as seen from Fig. 1b. Such wasteage may cause environmental hazards. To the best of our knowledge, there has been no publication on the effective utilization of waste LLS for high value-added products apart from a recent study by Liu *et al.* (2012) on the manufacture of lotus stalk-derived activated carbons.

Fig. 1. Photographs of (a) lotus plant, (b) withered lotus leaf stalks decaying in a wetland, (c) dry powders of raw lotus leaf stalks, and (d) freeze-dried bleached lotus leaf stalk (BLLS) filter cake

To better utilize LLS waste, an evaluation of LLS as a non-woody plant fiber source for the production of nanocelluloses deserves a systematic investigation. Controlled sulfuric acid hydrolysis is a well-known process used for isolation of nanocelluloses because of the colloidal stability of the resulting negatively charged suspensions. Moreover, the ultrasonic-assisted acid hydrolysis process has been successfully applied for the extraction of nanocelluloses with higher efficiency and with more uniform morphologies compared to the conventional acid hydrolysis in the absence of ultrasonication. This success may be attributed to the intensified diffusion of the acid under ultrasound irradiation to improve the accessibility and reactivity of the cellulose (Tang *et al*. 2005; Li *et al*. 2011; Tang *et al*. 2011; Lu *et al*. 2013).

In addition, high-intensity ultrasonication offers great potential for environmentally friendly disintegration of chemically purified fibers into nanofibers with superior lengths (Chen *et al*. 2011a,b) in comparison with nanowhiskers isolated by the acid hydrolysis method. The present study reports, for the first time, the isolation of cellulose nanofibers from LLS using a high-intensity ultrasonication technique. The chemical composition, microscopic morphology, crystalline behavior, and thermal properties of LLS and chemically purified LLS fibers were also characterized and are compared in detail.

EXPERIMENTAL

Materials

Raw materials and chemicals

The lotus leaf stalks (LLS) were collected from a constructed wetland located in Fuzhou, China. After harvest, the stems of the lotus plants were separated and then washed several times with deionized water. The cleaned biomass was dried at 100 °C for 24 h. The as-dried LLS were cut into pieces and subsequently ground in a mill equipped with a 40-mesh sieve to obtain powder samples. Then, the powder was sealed in polyethylene bags and stored in a desiccator until use. All chemicals used in the experiments were of analytical grade and used as received without further purification.

Methods

Extraction of pristine lotus leaf stalk cellulose

Chemically purified cellulose was isolated from LLS using a slightly modified three-step process that was described by Jiang and Hsieh (2013). Initially, the LLS powder was subject to a 2:1 volumetric ratio (v/v) of toluene/ethanol mixture extraction (90 °C, 6 h). After this treatment, the powder was bleached with an acidified $NaClO_2$ solution (2.0 wt%) at pH 4 for delignification (75 °C, 1 h); this process was repeated five times.

The residue obtained was washed thoroughly with distilled water, and the solid was termed holocellulose. After that, the resulting holocellulose fibers were further treated with 5.0 wt% KOH at 90 °C for 2 h to remove hemicelluloses. This treatment was followed by treatment with 1.0 wt% HCl solution at 80 °C for 2 h to yield highly purified acid-treated LLS cellulose fibers. At the end of the extraction, the obtained residue (α-cellulose) was recovered by filtration, washed with distilled water, and freeze-dried. The bleached cellulosic product thus obtained was referred to as bleached lotus leaf stalk (BLLS).

Preparation of nanocellulose defibrillated by high-intensity ultrasonication

The obtained highly purified BLLS was swelled overnight in 100 mL of distilled water at approximately 0.1 wt% solid content. The suspension was then subjected to a high frequency (20 to 25 kHz) ultrasound irradiation treatment in an ultrasonic generator equipped with a cylindrical alloy tip 1.5 cm in diameter (JY98-IIID type bio-cell disrupter, Ningbo Scientz Biotechnology Co., Ltd.; China) at an output power of 900 W. The ultrasonication was carried out in an icewater bath for 30 min, resulting in a suspension containing LLS-based nanofibrillated cellulose (NFC). The sonicated suspension was then centrifuged to collect NFC from the supernatant fraction.

Chemical composition

The content of moisture, ash, extractives, lignin, holocellulose, and alpha-cellulose was measured in the raw LLS as described in TAPPI standards (TAPPI T412 om-11 (2011a), TAPPI T211 om-07 (2007a), TAPPI T204 cm-07 (2007b), TAPPI T222 om-11 (2011b), TAPPI T9 m-54 (1998), and TAPPI T203 cm-09 (2009)). The difference between the values of holocellulose and α-cellulose gives the hemicellulose content of the fibers. Three replicates were tested for each sample, and average values were obtained. The results are presented in terms of dry mass.

Optical microscopy (OM) and MorFi analysis

The morphology of BLLS was observed using an optical microscope (XWY-VI, Hualun Papermaking Technology Co., Ltd.; Zhuhai, China) attached to a digital imaging system. One drop of a diluted suspension of BLLS was placed on a glass slide, and this was covered with a coverslip for OM observation.

The lengths and diameters of bleached fibers were determined automatically using a Techpap MorFi Compact fiber analyzer (Techpap, France). A set of at least 5000 fibers was analyzed during each MorFi run.

Fourier transform infrared spectroscopy (FTIR)

The FTIR spectra were recorded on a Nicolet AVATAR 360 spectrophotometer (Nicolet, USA) with a resolution of 4 cm^{-1} within the wave number range of 400 to 4000 cm^{-1}. The dried samples were ground and then blended with KBr at a ratio of about 1:100 prior to being pressed into pellets for analysis.

Transmission electron microscopy (TEM)

The nanostructure of the generated nanocellulose was measured using a FEI Tecnai G2 electron microscope (FEI, USA) operating at an acceleration voltage of 80 kV. Approximately 10 µL of diluted nanocellulose aqueous suspension was deposited on a copper grid with carbon film support and allowed to air dry. The samples stained with a 2% phosphotungstic acid solution were observed with the TEM once the grids dried at room temperature.

X-ray diffraction (XRD)

X-ray diffraction analysis was performed on an X'Pert Pro MPD X-ray diffractometer (Panalytical, Netherlands) with a Co tube at 40 kV and 30 mA. The crystallinity index (*CrI*) of the cellulose was calculated using Eq. (1) (Segal *et al*. 1959).

$$CrI = [(I_{002}\text{-}I_{am})/I_{002}] \times 100 \quad (1)$$

In this equation, I_{am} represents the minimal diffraction intensity of the amorphous region at a 2θ angle between 21° and 22°, and I_{002} is the maximum lattice diffraction intensity at a 2θ angle between 26°and 27° (Morais *et al*. 2013).

Thermogravimetric analysis (TGA)

The thermal stability of each sample was evaluated using a thermogravimetric analyzer (STA449C/4/G; Netzsch, Germany) at a heating rate of 10 °C·min^{-1} from 30 to 800 °C in a nitrogen atmosphere with a gas flow of 30 mL·min^{-1}.

RESULTS AND DISCUSSION

Chemical Analysis and Morphological Characteristics

The chemical constituents of LLS samples are listed in Table 1. The pristine LLS had 34.6% α-cellulose, which is within the normal range for other non-woody lignocellulosic sources, such as corn stover (33%), kenaf fibers (36%), wheat straw (30%) (Brinchi *et al*. 2013), coconut husk (32.5%) (Morais *et al*. 2013), and rice hulls (31%) (Adel *et al*. 2010). It also contained a considerable amount of lignin (25.4%), but its ash content was much lower (5.7%) than those of rice hulls (20.44%) and sugar beet (17.67%) (Li *et al*. 2014). To extract highly purified cellulose fibers from LLS, acid-chlorite and dilute alkali pretreatments were carried out. Furthermore, HCl treatment was employed to remove the alkali insoluble mineral components. The brown color of the original LLS powders (Fig. 1c) completely changed to a snow-white appearance after bleaching (Fig. 1d), indicating the highly effective removal of non-cellulosic components such as hemicellulose, lignin, wax, and extractives from the matrix during the treatment stages. The cellulose content in BLLS sample was thus evidently enriched with a content of 91.86% (by dry mass), resulting in highly purified LLS native cellulose suitable for the isolation of nanocelluloses.

Table 1. Compositional Analysis of Raw Lotus Leaf Stalks (LLS)

Component	Content (%, w/w)
Moisture	8.0
Ashes	5.7
Extractives	5.1
Lignin	25.4
Holocellulose	53.8
α-cellulose	34.6
Hemicellulose	19.2

Optical microscope analysis and MorFi analysis were adopted to investigate the morphological characteristics of the chemically treated LLS fibers. As shown in Fig. 2, the highly purified BLLS fibers were agglomerated, appearing as rigid rods with micron-scale dimensions. The average properties of BLLS fiber were further determined with a MorFi fiber analyzer, which is capable of rapid and reliable on-line and off-line fiber analysis for width and length distributions, kink, curl, and data on other fiber properties (Guay *et al*. 2005; Moral *et al*. 2010).

Figures 3a and 3b display length and width distribution diagrams of BLLS fibers calculated by MorFi analysis. The diameters of BLLS fibers were mostly distributed in the range of 20 to 60 μm, giving rise to an average diameter of 33.3 μm. The distribution of fiber lengths was less scattered in comparison with that of diameters. A total of 85.2% of the BLLS fibers had fiber weighted mean lengths ranging from 200 to 680 μm. The length-weighted average fiber length for BLLS was calculated as 460 μm.

The data in Table 2 show the typical average fiber characteristics of BLLS and reported whole wood pulps (Robertson *et al*. 1999), indicating that the selected average properties of BLLS fiber are much closer to those of hardwood pulp, and much lower in value compared to softwood pulp (Robertson *et al*. 1999).

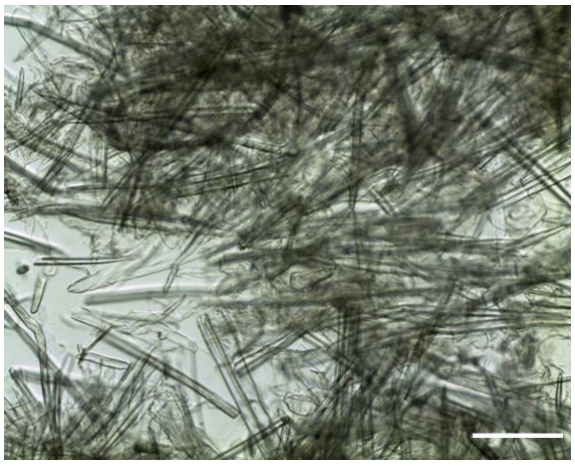

Fig. 2. Chemically purified lotus leaf stalk fibers (BLLS) observed in an optical microscope using a 100× objective lens. The scale bar equals 200 μm.

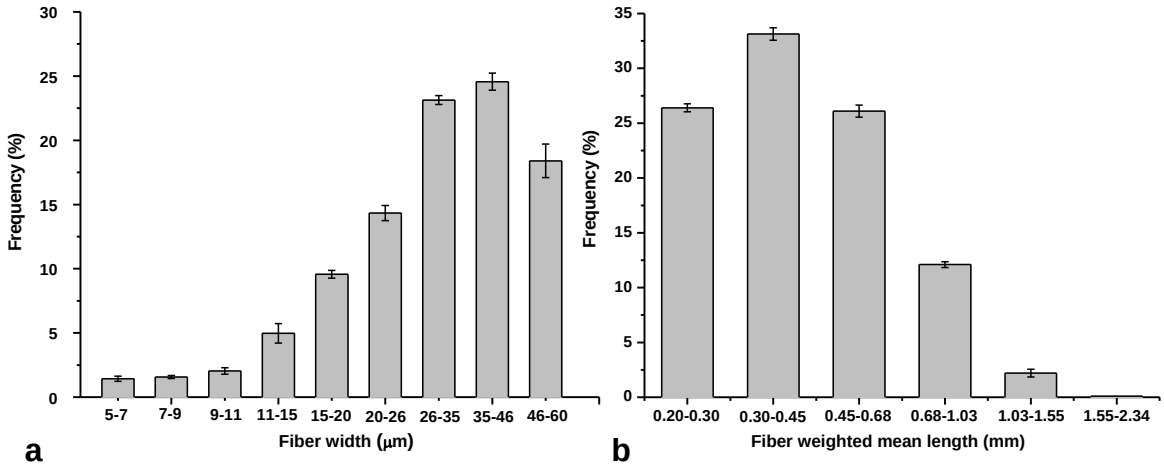

Fig. 3. The width (a) and length-weighted mean fiber length (b) distributions for BLLS measured by MorFi analyzer. Data provided as the mean ± standard deviation.

Table 2. Comparison of Average Characteristics of BLLS Fibers and Wood Pulps

Grand mean value	BLLS	Hardwood Pulp[1]	Softwood Pulp[1]
Fiber weighted mean length (mm)	0.46	0.65	2.22
Coarseness (mg/m)	0.072	0.085	0.140
Curl index	0.087	0.070	0.125

[1]Data from Robertson *et al*. 1999

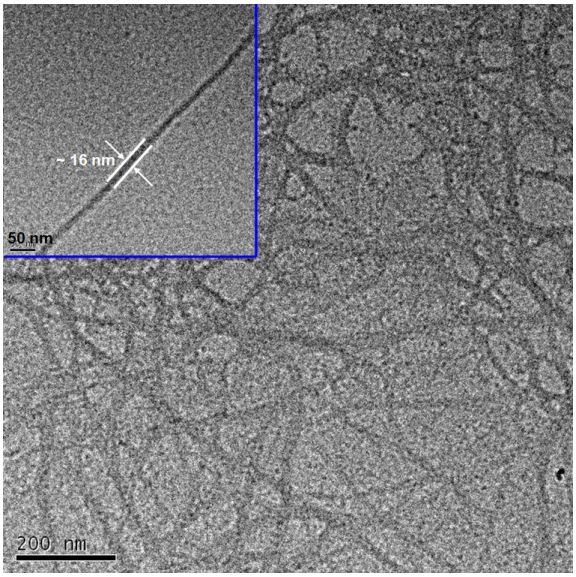

Fig. 4. Transmission electron micrograph of nanofibrillated cellulose (NFC) from BLLS

The nano-scale dimensions of the obtained NFC disintegrated *via* the high-intensity ultrasonication process were confirmed by TEM observations. The TEM image in Fig. 4 clearly reveals slender wire-like cellulose fibrils with nano-sized widths entangled in a network-like assembly of cellulose nanofibril agglomerations. As observed by TEM, most of the defibrillated nanofibrils had estimated widths of about 20 ± 5 nm and lengths on the micron scale, with an expected aspect ratio of approximately 40, which is extremely favorable for the anisotropic reinforcing effect and for network formation at low threshold during composite manufacturing (Chirayil *et al*. 2014). The formation of a network structure of NFC aggregates may be correlated with the high specific area and strong hydrogen bonds arising from the large number of hydroxyl groups exposed after high-intensity ultrasonication. The relatively shorter NFC obtained in the present work, as compared with the millimeter-scale NFC from bamboo fibers using the same method (Chen *et al*. 2011b), could be due to the inferior average fiber length of the pristine BLLS fiber, as measured by MorFi analysis. From the TEM results, it can be concluded that BLLS cellulose can be successfully refined to nano-scale dimensions with a large aspect ratio using the facile physical ultrasound defibrillation technique.

FTIR Analysis

Figure 5 compares the FTIR spectra of LLS, BLLS, and NFC. For all samples, the characteristic peaks of O-H stretching and C-H stretching centered at 3420 cm^{-1} and 2920 cm^{-1} were observed. In addition, the increased intensity of 3420 cm^{-1} absorption peak of BLLS and NFC in comparison with the raw LLS suggests that more free hydroxyl groups were exposed in the cellulose structure during the successive treatments (Abraham *et al*. 2013). The band at about 900 cm^{-1} can be ascribed to the deformation characteristic of the glycosidic linkage in cellulose (Adel *et al*. 2010; Jiang and Hsieh 2013). Furthermore, some peaks in the 600 to 900 cm^{-1} region associated with the aromatic ring C–H out of plane bending vibration were found in Fig. 5a for LLS, and those were not seen or appeared weaker for BLLS and NFC due to the removal of lignin by the sequentially chemical and sono-chemical treatments. The peak at 1510 cm^{-1} was found in the

spectrum of LLS, corresponding to the aromatic skeletal vibration in lignin. The band near 1245 cm^{-1} may be assigned to the deformation of the guaiacyl ring associated with C-O stretching in lignin, as well as to the axial asymmetric strain of =C-O-C bonds (Henrique *et al*. 2013). Hemicelluloses present in the raw LLS gave a dominant absorption band at 1740 cm^{-1}, representing the stretching of C=O groups (Elanthikkal *et al*. 2010; Abraham *et al*. 2013). These peaks almost disappeared in the BLLS spectra, verifying the efficient elimination of hemicelluloses and lignin by chemical treatment. These results are consistent with the chemical composition analysis depicted in Table 1. The spectrum of NFC was quite similar to that of BLLS, suggesting that no other chemical reaction occurred during the process of ultrasonic defibrillation.

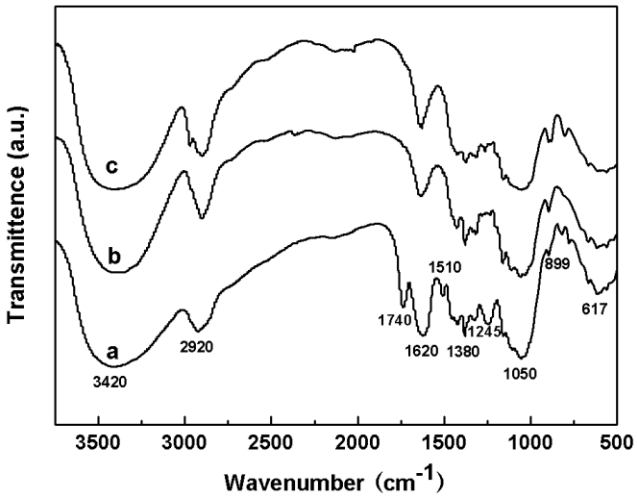

Fig. 5. Typical FTIR spectra obtained from (a) LLS, (b) BLLS, and (c) NFC

X-ray Diffraction Studies

The XRD patterns for LLS, BLLS, and NFC are shown in Fig. 6. The overall shape of all diffraction data is quite similar, presenting a remarkable predominance of cellulose component. The final NFC sample as well as BLLS exhibits the well-known diffraction peaks for 110, 200, and 004 crystallographic planes, which are the characteristic peaks of cellulose I lattice (Flauzino Neto *et al*. 2013; Tang *et al*. 2014). The crystallinity index (*CrI*) of LLS, BLLS, and NFC was calculated as 52%, 73%, and 70%, respectively, according to Segal's empirical method (Segal *et al*. 1959). The *CrI* value of BLLS was clearly increased, by 40%, with respect to LLS, most likely because of the effective removal of essentially amorphous non-cellulose constituents during the delignification and bleaching processes. After strong ultrasonic defibrillation, a slight decrease in the crystallinity of NFC compared to that of BLLS was observed. This may be due to the non-selective ultrasonication effect (Li *et al*. 2012b). As a result of the ultrasonic cavitation effect, not only the amorphous regions, but also the crystalline domains in the cellulose structure were subjected to severe physical disruption resulting from numerous cavitation-caused liquid jets with tremendous force (Cintas and Luche 1999), thereby causing the disintegration of BLLS to NFC with gently decreased crystallinity. However, the NFC still had a higher apparent crystallinity, *i.e.*, 70%, compared to the value of 61.25% for the NFC isolated from bamboo fibers in the previous report using the same method (Chen *et al*. 2011b). The high crystallinity of NFC suggests a great potential for use as a green reinforcement in composites.

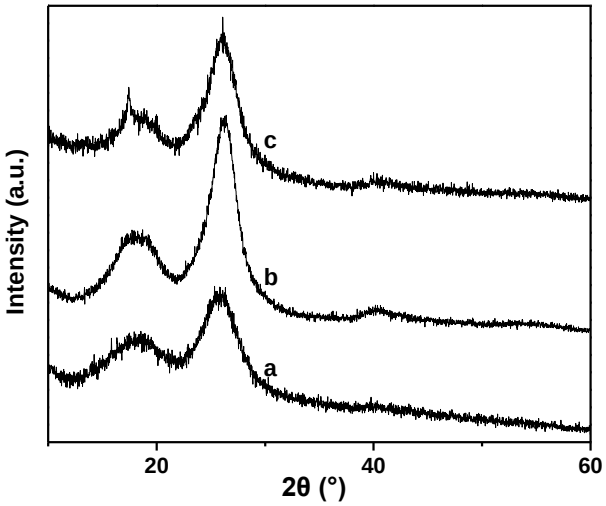

Fig. 6. X-ray diffractograms from (a) LLS, (b) BLLS, and (c) NFC

Thermal Analysis

The TG and DTG curves of the LLS, BLLS, and NFC are shown in Figs. 7A and B, respectively. In all cases, a small weight drop related to the moisture was found at approximately 50 to 120 °C, and one major degradation stage was observed. When heated to 500 °C, smaller amounts of carbonized residues were left behind for BLLS and NFC when compared to LLS. This is because the purification treatment effectively removed the non-cellulosic constituents that could induce higher char formation (Neto *et al*. 2013; Li *et al*. 2014).

Overall, the thermal degradation data depicted in Fig. 7B show conclusively that BLLS and NFC had a better thermal stability than the raw LLS. This can be attributed to the removal of substantial amounts of cementing materials, such as hemicellulose, lignin, and starch, with low initial decomposition temperature (Henrique *et al*. 2013). The DTG profile of raw LLS exhibited a small broadening on the left side of the main peak, presenting an initial decomposing temperature (T_i) and temperature at maximum decomposing (T_{max}) of 190 and 311 °C, respectively. In the case of BLLS, T_i increased to 275 °C, with the rate of degradation maximized at 332 °C.

Although the NFC started to degrade at around 217 °C, the dominant DTG peak moved to approximately 344 °C. The lower T_i of NFC could be ascribed to the nano-scale fiber dimensions as compared to the macroscopic cellulose fibers, which lead to increased accessible surface area for thermal decomposition (Li *et al*. 2012b; Zhao *et al*. 2013).

Additionally, damage in the crystal regions between cellulose resulting in reduced crystallinity after the ultrasonication can be expected to cause the early onset of degradation for NFC (Li *et al*. 2012a). These thermal analysis results are in agreement with the chemical composition, XRD, and FTIR results. The good thermal stability of the as-prepared NFC may improve its applicability as a biocompatible material, especially at the temperatures higher than 200 °C (Li *et al*. 2014).

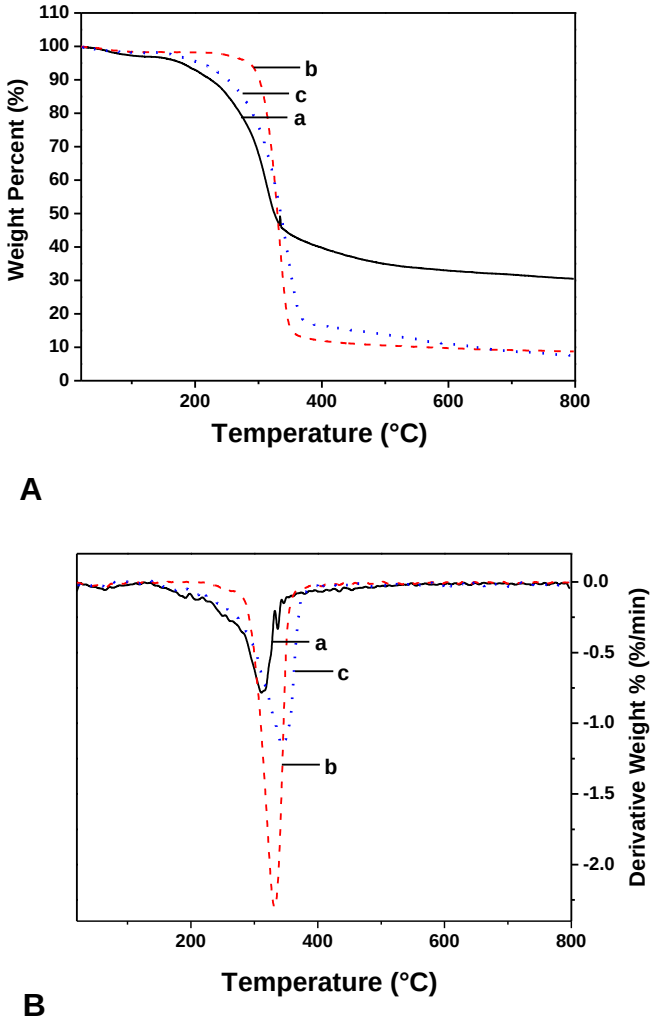

Fig. 7. (A) TG and (B) DTG curves for (a) LLS, (b) BLLS, and (c) NFC

CONCLUSIONS

1. Fibers from lotus leaf stalk (LLS) agro-waste were isolated and characterized. The primary component of the chemically purified fibers was cellulose, presenting LLS cellulose fibers with diameters mostly in the range of 20 to 60 μm, as verified by OM and MorFi fiber analysis.
2. The upgrading of LLS fibers to value-added nanofibrillated cellulose (NFC) can be achieved *via* conventional chemical pretreatment followed by the purely physical defibrillation process of high-intensity ultrasonication.
3. Individual NFC that appeared in TEM images was of a slender wire-like material with uniform diameters of 20 ± 5 nm and lengths on the micron scale, giving rise to an aspect ratio of approximately 40 that was linked in a network structure. Moreover, the extracted BLLS fibers and NFC showed enhanced crystallinity and thermal stability.
4. This work provides a basis for further exploitation of these cellulosic fibers.

ACKNOWLEDGMENTS

This work was financially supported by the National Natural Science Foundation of China (No. 31000276 and 31170520) and the Fundamental Research Funds for Distinguished College Young Scholars of Fujian Province, China (No. JA11071 and No. JA12088). We also gratefully acknowledge financial funding from the Incubation Program for Distinguished Young Scholars of FAFU Science Foundation (No. xjq201208).

REFERENCES CITED

Abraham, E., Deepa, B., Pothen, L. A., Cintil, J., Thomas, S., John, M. J., and Narine, S. S. (2013). "Environmental friendly method for the extraction of coir fibre and isolation of nanofibre," *Carbohydrate Polymers* 92(2), 1477-1483. DOI: 10.1016/j.carbpol.2012.10.056

Adel, A. M., El-Wahab, Z. H. A., Ibrahim, A. A., and Al-Shemy, M. T. (2010). "Characterization of microcrystalline cellulose prepared from lignocellulosic materials. Part I. Acid catalyzed hydrolysis," *Bioresource Technology* 101(12), 4446-4455. DOI: 10.1016/j.biortech.2010.01.047

Brinchi, L., Cotana, F., Fortunati, E., and Kenny, J. M. (2013). "Production of nanocrystalline cellulose from lignocellulosic biomass: Technology and applications," *Carbohydrate Polymers* 94(1), 154-169. DOI: 10.1016/j.carbpol.2013.01.033

Chen, W., Yu, H., Li, Q., Liu, Y., and Li, J. (2011a). "Ultralight and highly flexible aerogels with long cellulose I nanofibers," *Soft Matter* 7(21), 10360-10368. DOI: 10.1039/C1SM06179H

Chen, W., Yu, H., and Liu, Y. (2011b). "Preparation of millimeter-long cellulose I nanofibers with diameters of 30-80 nm from bamboo fibers," *Carbohydrate Polymers* 86(2), 453-461. DOI: 10.1016/j.carbpol.2011.04.061

Cheng, L., Li, S., Yin, J., Li, L., and Chen, X. (2013). "Genome-wide analysis of differentially expressed genes relevant to rhizome formation in lotus root (*Nelumbo nucifera* Gaertn)," *PloS One* 8(6), e67116. DOI: 10.1371/journal.pone.0067116

Chirayil, C. J., Joy, J., Mathew, L., Mozetic, M., Koetz, J., and Thomas, S. (2014). "Isolation and characterization of cellulose nanofibrils from *Helicteres isora* plant," *Industrial Crops and Products* 59, 27-34. DOI: 10.1016/j.indcrop.2014.04.020

Cintas, P., and Luche, J. L. (1999). "Green chemistry. The sonochemical approach," *Green Chemistry* 1(3), 115-125. DOI: 10.1039/A900593E

Eichhorn, S. J. (2011). "Cellulose nanowhiskers: Promising materials for advanced applications," *Soft Matter* 7(2), 303-315. DOI: 10.1039/C0SM00142B

Elanthikkal, S., Unnikrishnan, G., Varghese, S., and Guthrie, J. T. (2010). "Cellulose microfibers produced from banana plant wastes: isolation and characterization," *Carbohydrate Polymers* 80, 582-859. DOI:10.1016/j.carbpol.2009.12.043

Flauzino Neto, W. P., Silvério, H. A., Dantas, N. O., and Pasquini, D. (2013). "Extraction and characterization of cellulose nanocrystals from agro-industrial residue–soy hulls," *Industrial Crops and Products* 42, 480-488. DOI:10.1016/j.indcrop.2012.06.041

Guay, D., Sutherland, N. R., Rantanen, W., Malandri, N., Stephens, A., Mattingly, K., and Point, U. S. (2005, May). "Comparison of fiber length analyzers," *TAPPI Practical Papermaking Conf. May*, pp. 22-26.

Haafiz, M. K., Hassan, A., Zakaria, Z., and Inuwa, I. M. (2014). "Isolation and characterization of cellulose nanowhiskers from oil palm biomass microcrystalline cellulose," *Carbohydrate Polymers* 103, 119-125. DOI: 10.1016/j.carbpol.2013.11.055

Henrique, M. A., Silvério, H. A., Flauzino Neto, W. P., and Pasquini, D. (2013). "Valorization of an agro-industrial waste, mango seed, by the extraction and characterization of its cellulose nanocrystals," *Journal of Environmental Management* 121, 202-209. DOI: 10.1016/j.jenvman.2013.02.054

Jiang, F., and Hsieh, Y. L. (2013). "Chemically and mechanically isolated nanocellulose and their self-assembled structures," *Carbohydrate Polymers* 95(1), 32-40. DOI: 10.1016/j.carbpol.2013.02.022

Klemm, D., Kramer, F., Moritz, S., Lindström, T., Ankerfors, M., Gray, D., and Dorris, A. (2011). "Nanocelluloses: A new family of nature-based materials," *Angewandte Chemie International Edition* 50(24), 5438-5466. DOI: 10.1002/anie.201001273

Li, W., Wang, R., and Liu, S. (2011). "Nanocrystalline cellulose prepared from softwood kraft pulp via ultrasonic-assisted acid hydrolysis," *BioResources* 6(4), 4271-4281. DOI: 10.15376/biores.6.4.4271-4281

Li, J., Wei, X., Wang, Q., Chen, J., Chang, G., Kong, L., and Liu, Y. (2012a). "Homogeneous isolation of nanocellulose from sugarcane bagasse by high pressure homogenization," *Carbohydrate Polymers* 90(4), 1609-1613. DOI: 10.1016/j.carbpol.2012.07.038

Li, W., Yue, J., and Liu, S. (2012b). "Preparation of nanocrystalline cellulose via ultrasound and its reinforcement capability for poly (vinyl alcohol) composites," *Ultrasonics Sonochemistry* 19(3), 479-485. DOI: 10.1016/j.ultsonch.2011.11.007

Li, M., Wang, L. J., Li, D., Cheng, Y. L., and Adhikari, B. (2014). "Preparation and characterization of cellulose nanofibers from de-pectinated sugar beet pulp," *Carbohydrate Polymers* 102, 136-143. DOI: 10.1016/j.carbpol.2013.11.021

Lin, N., and Dufresne, A. (2014). "Nanocellulose in biomedicine: Current status and future prospect," *European Polymer Journal* 59, 302-325. DOI: 10.1016/j.carbpol.2013.11.021

Liu, H., Zhang, J., Bao, N., Cheng, C., Ren, L., and Zhang, C. (2012). "Textural properties and surface chemistry of lotus stalk-derived activated carbons prepared using different phosphorus oxyacids: Adsorption of trimethoprim," *Journal of Hazardous Materials* 235, 367-375. DOI: 10.1016/j.jhazmat.2012.08.015

Lu, Z., Fan, L., Zheng, H., Lu, Q., Liao, Y., and Huang, B. (2013). "Preparation, characterization and optimization of nanocellulose whiskers by simultaneously ultrasonic wave and microwave assisted," *Bioresource Technology* 146, 82-88. DOI: 10.1016/j.biortech.2013.07.047

Man, J., Cai, J., Cai, C., Xu, B., Huai, H., and Wei, C. (2012). "Comparison of physicochemical properties of starches from seed and rhizome of lotus," *Carbohydrate Polymers* 88(2), 676-683. DOI: 10.1016/j.carbpol.2012.01.016

Morais, J. P. S., Rosa, M. D. F., Nascimento, L. D., do Nascimento, D. M., and Cassales, A. R. (2013). "Extraction and characterization of nanocellulose structures from raw cotton linter," *Carbohydrate Polymers* 91(1), 229-235. DOI: 10.1016/j.carbpol.2012.08.010

Moral, A., Concepción Monte, M., Cabeza, E., and Blanco, A. (2010). "Morphological characterisation of pulps to control paper properties," *Cellulose Chemistry & Technology* 44(10), 473-480.

Neto, W. P. F., Silvério, H. A., Dantas, N. O., and Pasquini, D. (2013). "Extraction and characterization of cellulose nanocrystals from agro-industrial residue – Soy hulls," *Industrial Crops and Products* 42, 480-488. DOI: 10.1016/j.indcrop.2012.06.041

Robertson, G., Olson, J., Allen, P., Chan, B., and Seth, R. (1999). "Measurement of fiber length, coarseness, and shape with the fiber quality analyzer," *TAPPI Journal* 82(10), 93-98.

Segal, L., Creely, J. J., Martin Jr., A. E., and Conrad, C. M. (1959). "An empirical method for estimating the degree of crystallinity of native cellulose using the X-ray diffractometer," *Textile Research Journal* 29(10), 786-794. DOI: 10.1177/004051755902901003

Tang, A. M., Zhang, H. W., Chen G., Xie G. H., and Liang, W. Z. (2005). "Influence of ultrasound treatment on accessibility and regioselective oxidation reactivity of cellulose," *Ultrasonics Sonochemistry* 12(6), 467-472.

Tang, L. R., Huang, B., Ou, W., Chen, X. R., and Chen, Y. D. (2011). "Manufacture of cellulose nanocrystals by cation exchange resin-catalyzed hydrolysis of cellulose," *Bioresource Technology* 102(23), 10973-10977. DOI: 10.1016/j.biortech.2011.09.070

Tang, Y., Yang, S., Zhang, N., and Zhang, J. (2014). "Preparation and characterization of nanocrystalline cellulose via low-intensity ultrasonic-assisted sulfuric acid hydrolysis," *Cellulose 21*(1), 335-346. DOI: 10.1007/s10570-013-0158-2

TAPPI T9 m-54. (1998). "Holocellulose in wood," *TAPPI Press,* Atlanta, GA.

TAPPI T203 cm-09. (2009). "Alpha-, beta- and gamma-cellulose in pulp," *TAPPI Press,* Atlanta, GA.

TAPPI T204 cm-07. (2007b). "Solvent extractives of wood and pulp," *TAPPI Press,* Atlanta, GA.

TAPPI T211 om-07. (2007a). "Ash in wood, pulp, paper, and paperboard: Combustion at 525 °C," *TAPPI Press,* Atlanta, GA.

TAPPI T222 om-11. (2011b). "Acid-insoluble lignin in wood and pulp," *TAPPI Press,* Atlanta, GA.

TAPPI T412 om-11. (2011a). "Moisture in pulp, paper and paperboard," *TAPPI Press,* Atlanta, GA.

Xu, L., Shi, P. T., Ye, Z. H., Yan, S. M., and Yu, X. P. (2013). "Rapid analysis of adulterations in Chinese lotus root powder (LRP) by near-infrared (NIR) spectroscopy coupled with chemometric class modeling techniques," *Food Chemistry* 141(3), 2434-2439. DOI: 10.1016/j.foodchem.2013.05.104

Zhao, J., Zhang, W., Zhang, X., Zhang, X., Lu, C., and Deng, Y. (2013). "Extraction of cellulose nanofibrils from dry softwood pulp using high shear homogenization," *Carbohydrate Polymers* 97(2), 695-702. DOI: 10.1016/j.carbpol.2013.05.050

Article submitted: September 15, 2014; Peer review completed: November 19, 2014; Revisions accepted: November 25, 2014; Published: December 3, 2014.